

Separation of flow from chiral magnetic effect in U+U collisions using spectator asymmetry

Sandeep Chatterjee* and Prithwish Tribedy†

Variable Energy Cyclotron Centre, 1/AF Bidhannagar, Kolkata, 700064, India

Abstract

We demonstrate that the prolate shape of the Uranium nucleus generates anti-correlation between spectator asymmetry and initial state ellipticity of the collision zone, providing a way to constrain the initial event shape in U+U collisions. As an application, we show that this can be used to separate the background contribution due to flow from the signals of chiral magnetic effect.

The hot and dense QCD plasma produced in heavy ion collisions (HIC) can give rise to metastable vacuum with non trivial topology of the gauge field configurations like sphalerons and instantons. These give rise to P and CP odd interactions between quark and gluon fields that change the quark chirality [1, 2]. In the early stages of HICs, strong magnetic fields $\sim m_\pi^2$ are expected to be produced [3–5]. This unique combination of local P and CP odd domains amidst strong magnetic field in HIC experiments is expected to give rise to many interesting phenomena like the chiral magnetic effect (CME) [6]. The separation of charged hadrons along the direction of the magnetic field has been suggested as a possible signal of CME in which the like sign charges are expected to be emitted in the same direction [2]. However, such angular correlations can also arise due to non-CME effects like elliptic flow, resonance decays, momentum conservation kinematics etc [7]. In order to reduce the non-flow effects, the following charged particle correlator was proposed in Ref. [8]

$$\gamma^{ab} = \langle \cos(\phi^a + \phi^b - 2\psi_{RP}) \rangle. \quad (1)$$

Here ϕ is the azimuthal angle of the particle and $a, b = \pm$, is its charge state. ψ_{RP} is the reaction plane angle. The non-flow effects that are random with respect to the reaction plane are eliminated by the design of this observable. It is however difficult to reduce the background from elliptic flow. The elliptic flow v_2 is largely characterised by the initial shape of the collision zone and the strength of CME signal depends on the number of spectators. It turns out that the attempts to reduce flow, say by going towards central events, also reduces the magnetic field and therefore the signal of CME due to decrease in the number of spectators. Therefore, although γ^{ab} has been measured in Au+Au, Cu+Cu and Pb+Pb collisions [9–12], the final verdict on CME is still not out. This is mainly because it is not possible to separate the background flow effects from γ^{ab} unambiguously by conventional approaches [13].

There have been suggestions on disentangling the CME from flow [14, 15]. In Au+Au collisions, it has been suggested that within a narrow centrality bin large fluctuation of the initial state ellipticity produces a broad event by event distribution of v_2 while CME is expected to be nearly constant because of similar number of spectators [15], thereby disentangling the two effects.

The other approach is to study the collisions of deformed nucleus such as Uranium [14]. It has been pointed out that in full overlap U+U collisions, the magnetic field in the overlap zone nearly vanishes, although a large anisotropy is generated from certain configurations of the prolate shape of the Uranium nucleus. This allows one to turn off CME while having substantial v_2 in such collisions [14].

In this work we propose a new method to systematically reduce the initial anisotropy that contributes to v_2 in a given sample of events without reducing the effect of magnetic field that generates the signals of CME in U+U collisions. For further discussions we introduce a quantity, the spectator nucleon asymmetry $|L - R|$ which is defined as the absolute difference between the left (L) and right (R) going nucleons that did not participate in the collision. In case of the collisions of non-deformed nuclei like Pb, the spherical shape of the individual nucleus ensures that $|L - R|$ receives no contribution from the collision geometry. The non-zero values of $|L - R|$ in such cases can arise only due to quantum fluctuations of the nucleon positions in the colliding nuclei. Here we will not focus on such initial state fluctuations. In the case of U+U collisions, $|L - R|$ receives a dominant contribution from the geometric fluctuations. We argue and demonstrate through Monte Carlo Glauber (MCG) simulations that $|L - R|$ is an important tuning parameter to constrain the initial state geometry in U+U collisions that can be useful for several purposes.

Deformed nuclear collisions are characterized by four angles representing the orientations of the major axes of the colliding nuclei in addition to the impact parameter b [14, 16–18]. They include the two polar angles Θ_1 and Θ_2 relative to the collision direction (z-axis) as shown in Fig. 1 and two azimuthal angles Φ_1 and Φ_2 in the plane transverse to the collision direction, the collision plane.

* sandeepc@vecc.gov.in

† ptribedy@vecc.gov.in

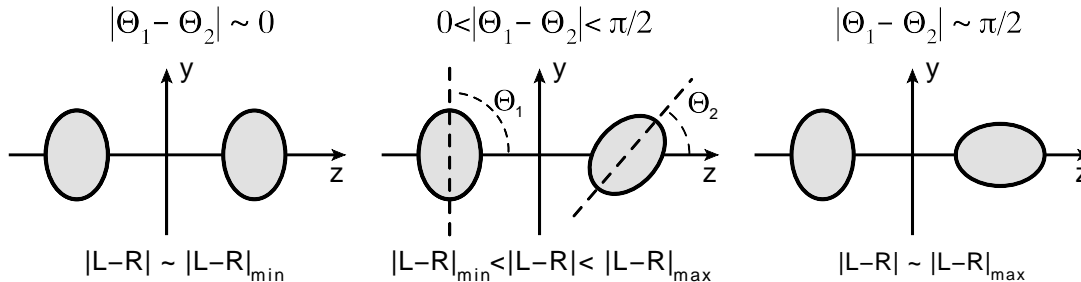


FIG. 1. Geometries of U+U collisions that generate higher spectator neutron asymmetry $|L - R|$ due to increase in the angle between the major axes of two nuclei at a fixed impact parameter. The collision direction is chosen along the z-axis.

There are collision configurations where both the nuclei have similar projected geometry on the collision plane as in the case of collisions of non-deformed nuclei. Such configurations are not expected to generate large spectator asymmetry. On the other hand, configurations in which one nucleus largely engulfs the other can generate higher values of $|L - R|$. In such configurations, there is a large difference in the projected geometry of the two nuclei on the collision plane. In Fig. 1 we demonstrate how $|L - R|$ changes with collision configurations. We start with a special configuration where both nuclei have the same values of Θ at a fixed b . In this configuration $|L - R|$ is generated solely due to nucleon scale quantum fluctuations. Thus, $|L - R|$ has a minimal value of say $|L - R|_{\min}$. As the difference in the projected geometry of the two nuclei grows with increasing polar angle difference ($|\Theta_1 - \Theta_2|$), we expect larger values of $|L - R|$. Finally, $|L - R|$ reaches a maximum value $|L - R|_{\max}$ when the major axis of one nucleus aligns along the collision direction while the other one is perpendicular to it. We call such configurations as Body-tip (or Side-tip) collisions. Due to prolate shape of Uranium nucleus, it is evident that such configurations will lead to smaller anisotropy of the overlap zone. We will demonstrate that in a given multiplicity bin, increasing $|L - R|$ leads to systematic decrease in ellipticity. It is interesting to note that in case of significant oblate deformation, an opposite behavior is expected- higher values of $|L - R|$ will lead to larger ellipticity. In HIC experiments, spectator neutrons from the left and right moving nuclei are measured by two Zero Degree Calorimeters (ZDC) while the spectator protons are never measured [19]. Therefore a quantity of experimental interest would be the asymmetry of spectator neutrons. Such a quantity can be easily measured in the experiment by measuring the energy depositions in the two ZDCs due to incident neutrons. In the remaining discussion, we will refer to $|L - R|$ as the spectator neutron asymmetry.

Minimum bias events (all values of impact parameter) for U+U and Au+Au collisions at 193 GeV and 200 GeV

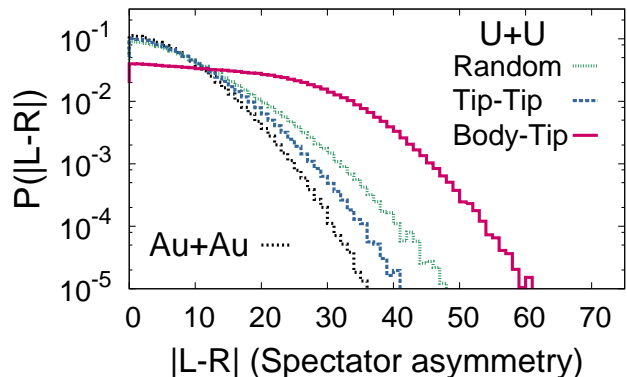


FIG. 2. (Color online) Probability distribution of spectator neutron asymmetry parameter $|L - R|$ for Au+Au and different configurations of U+U collisions.

respectively are generated using a two-component Monte-Carlo Glauber (MCG) model. The details of the Glauber model and the parameters of the Wood-Saxon distributions for the nuclei used here are the same as used in Ref. [20]. The free parameters of the MCG model that relates collision geometry to multiplicity have been tuned to reproduce the min-bias multiplicity distribution predicted by the IP-Glasma model as described in Ref. [20]. In Fig. 2, we plot the probability distributions of $|L - R|$ for Au+Au collisions and three different collision configurations of U+U. The Tip-Tip configuration corresponds to $\Theta_1 = \Theta_2 = 0$ and $\Phi_1 = \Phi_2 = 0$ and the Body-Tip configuration corresponds to $\Theta_1 = \pi/2, \Theta_2 = 0$ and $\Phi_1 = \Phi_2 = 0$. The “Random” configuration refers to unpolarized U+U collisions. For Au+Au collisions that include small oblate deformation, we do not find significant difference between specific orientations and only show the distribution for the unpolarized collisions.

The distributions for Au+Au and Tip-Tip U+U collisions correspond to smaller values of maximal $|L - R|$ as compared to random U+U configuration. This is because, in these cases, non-zero values of $|L - R|$ arise

purely from quantum fluctuations of the nucleon positions. The small difference in the probability distributions between these configurations is due to the larger number of nucleons in Uranium that broadens the probability distribution of $(L - R)$ itself. The Body-Tip configuration, as expected, produces the highest spectator neutron asymmetry. Thus as argued before and as shown in Fig. 2, in case of Random U+U collisions, events with highest values of $|L - R|$ are dominated by Body-Tip events. For the rest part of this paper, by U+U collisions we refer to “Random U+U” collisions.

We will now study the variation of ellipticity and CME like signal with $|L - R|$. In our calculation we define ellipticity (ε_2) as

$$\varepsilon_2 e^{i2\Psi_2^{PP}} = \frac{\sum_p r_p^2 e^{i2\phi_p}}{\sum_p r_p^2}, \quad (2)$$

where the sum is performed over the positions of participant nucleons (assumed to be delta-functions) at positions (r_p, ϕ_p) . Here Ψ_2^{PP} denotes the second order participant plane [21–24], a measure of the direction of the initial state spatial anisotropy. In order to serve as a proxy for the experimental event plane, that measures the final state momentum anisotropy, Ψ_2^{PP} is rotated by $\pi/2$ as per convention [23]. A similar plane can be defined using the positions of spectator neutrons (r_s, ϕ_s) in the collision plane as

$$\Psi_2^{SP} = \frac{1}{2} \tan^{-1} \left(\frac{\sum_s r_s^2 \sin 2\phi_s}{\sum_s r_s^2 \cos 2\phi_s} \right). \quad (3)$$

In experiment, the plane of spectator neutrons can be directly measured using ZDCs [11, 19].

The other quantity of interest is the correlation of the magnetic field B generated by the protons in the U nuclei with the reaction plane Ψ_{RP} defined as

$$\gamma^B = e^2 B^2 \cos(2(\Psi_B - \Psi_{RP})). \quad (4)$$

Here B is the magnitude and Ψ_B is the angle of the resultant B -field vector at the point of observation due to all protons. This correlator has been argued to serve as a proxy for the CME signal γ^{ab} [25, 26]. This quantity is similar to Eq.1 of γ^{ab} with $\phi_a + \phi_b$ replaced by $2\Psi_B$.

In this work we estimate the values of B and Ψ_B at the time of collision ($t = 0$) using the expression of Lienard-Wiechert potentials [4, 27, 28]. The estimates shown here are at the central point of the participant zone defined by the average weighted positions of the participants. We compute ε_2 and γ^B for different bins of $|L - R|$ in a given centrality class. The centrality selection in our case is done from the min-bias multiplicity distribution of U+U collisions.

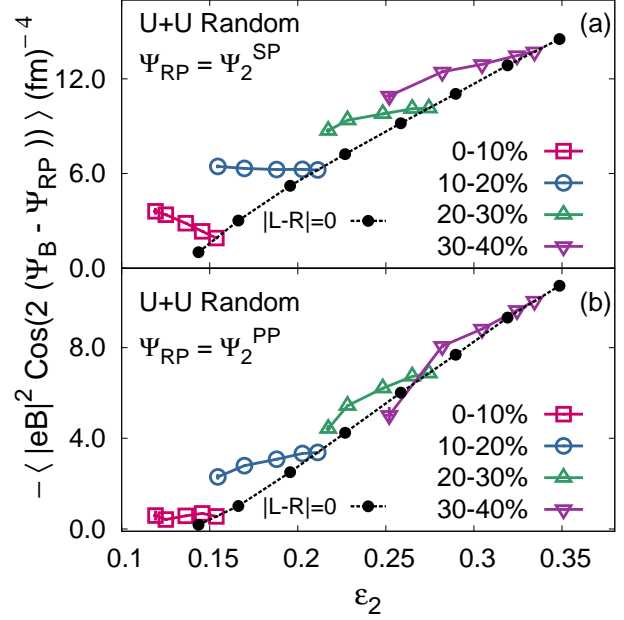


FIG. 3. (Color online) The correlator γ^B at the centre of the participant zone vs ε_2 for different centrality and spectator asymmetry bins. *Top*: γ^B measured with respect to the 2nd spectator plane. *Bottom*: γ^B measured with respect to the 2nd participant plane. Bins with same ε_2 is observed to have multiple γ^B and vice-versa.

In Fig. 3 we show the correlation between γ^B and ε_2 for different bins of centrality and $|L - R|$. We have used $\Psi_{RP} = \Psi_2^{SP}$ (Fig.3.(a)) and Ψ_2^{PP} (Fig.3.(b)). The centrality is varied in the range of 0 – 40% over which we expect ε_2 to be a good proxy for v_2 [29, 30]. The $|L - R| = 0$ bins for different centralities are shown by solid symbols. This indicates that γ^B proportionally increases with ε_2 for different centrality bins. Thus by changing the centralities alone it is not possible to disentangle CME from that of the collective response to ε_2 . An interesting behavior is seen by introducing the spectator asymmetry parameter which allows us to tune ε_2 in a given centrality class. The different points in a given centrality bin, shown by open symbols are obtained when $|L - R|$ is varied in the range of 0 to 45. In all the cases the different curves extend out from the $|L - R| = 0$ curve. This indicates that a given value of ε_2 corresponds to multiple values of γ^B and vice-versa. This is more prominent for the two most central bins (0 – 10) % and (10 – 20) % and much stronger when Ψ_2^{SP} is used as Ψ_{RP} .

We argue that this behavior can be the key to disentangle the effects of γ^B that drives γ^{ab} from initial ε_2 that drives v_2 . A correlation plot of γ^{ab} vs v_2 for different centralities for $|L - R| = 0$, similar to Fig.3 can be measured in the experiment. The next step would be to extract

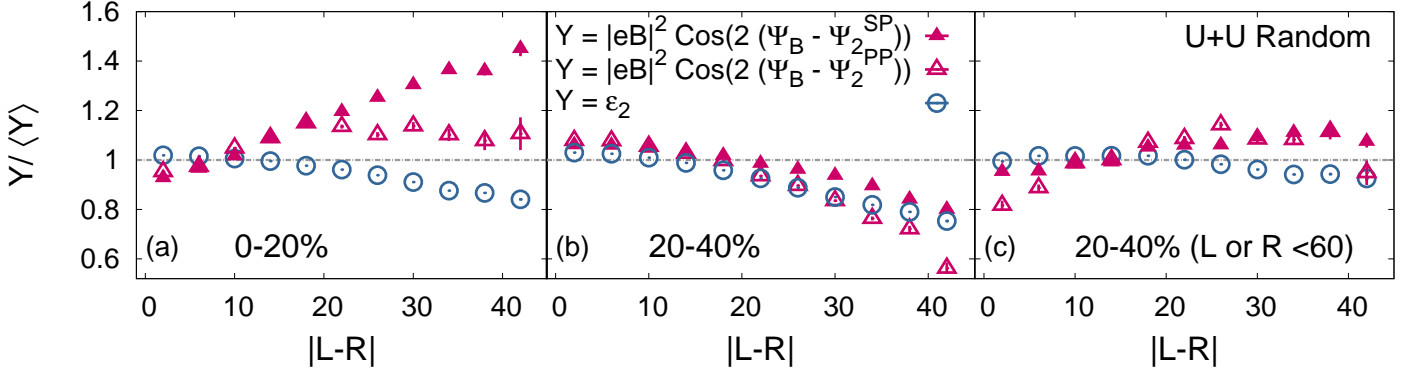


FIG. 4. (Color online) The initial state ε_2 and γ^B at the origin of the participant plane vs $|L - R|$ for different choices of ψ_{RP} , $\psi_{RP} = \psi_2^{PP}$ and ψ_2^{SP} . The plots are for (0 – 20) % and (20 – 40) % centrality cases. Panel (c) again shows the (20 – 40) % centrality class with additional cut on the maximum value of L or R

the same correlation by varying $|L - R|$ at a given centrality. If γ^{ab} is only sensitive to the variation in v_2 the two correlation curves will overlap. On the other hand, if γ^{ab} is driven by CME, one expects different slopes of the correlation curves as shown in Fig.3. In that case, a given value of v_2 will correspond to multiple values of γ^{ab} and vice-versa. Such observation will lead to a clear disentanglement between the two effects and a strong support for CME.

We note from Fig. 3 that there is a hint of anti-correlation between ε_2 and γ^B for the central collisions. This is clearly visible in Fig. 3 (a). We try to focus on this aspect more elaborately in Fig. 4. Here we have combined the two central bins (0 – 10) % and (10 – 20) % into a single bin of (0 – 20) % and the rest into another bin of (20 – 40) %. In each case we plot the variation of ε_2 and γ^B scaled by their mean values in a given centrality bin with respect to $|L - R|$. For both centralities, ε_2 monotonically decreases with increasing $|L - R|$ by about 20%. Interestingly, as shown in Fig.4 (a), for the (0 – 20) % centrality bin γ^B grows with increasing $|L - R|$. The growth is stronger when Ψ_2^{SP} is used for the estimation of event plane. In that case about 50% increase is observed. When Ψ_2^{PP} is used for the calculation, γ^B initially increases by about 20% and becomes nearly constant. Thus for the (0 – 20) % centrality bin, we find that by varying $|L - R|$ alone one can in principle observe anti-correlation between the effects of B -field that lead to CME-like signals and flow-like effects. However we find that for the (20 – 40) % centrality bin, both ε_2 and γ^B go down with increasing $|L - R|$. This is shown in Fig. 4 (b). This trend however drastically changes (as shown in Fig. 4 (c)) by restricting the number of spectators on any one side (L or R). We find that by applying a cut of L or R less than 60, once again we see a trend qualitatively similar to the (0 – 20) % bin. Such observation of anti-

correlation between γ^{ab} and v_2 in data will lead to a very strong case for CME.

The effects seen in Fig. 3 and Fig. 4 can be understood in the following way. As illustrated in Figs. 1 and 2, increasing $|L - R|$ in general increases the fraction of Body-Tip events thereby decreasing ε_2 in a multiplicity bin. This decrease of ε_2 with $|L - R|$ is a robust effect intrinsic to the prolate deformation of Uranium. However the strength of the projected B -field $e^2 B^2 \cos(2(\Psi_B - \Psi_{RP}))$ have a more complicated dependence on $|L - R|$. For the central collisions, increasing $|L - R|$ also results in increasing the number of spectators. This is because the smaller $|L - R|$ bins in central events are dominated by full overlap collisions with very few spectators compared to central Body-Tip events. Thus, a relative increase of spectators is obtained by increasing $|L - R|$. However, in the (20 – 40) % bin increasing $|L - R|$ does not necessarily increase the number of spectators. In this centrality, the smaller $|L - R|$ bins are already dominated by non-central collisions which have large number of spectators. Introduction of an additional cut on the number of spectators on either side L or R , once again leads to a relative increase of spectator and therefore an increase of γ^B with $|L - R|$.

In summary, we find that in U+U collisions the spectator neutron asymmetry $|L - R|$ gives us a direct access to the initial state geometry. It serves as a control parameter to trigger events with different values of initial anisotropy. This parameter can be experimentally measured by using a combination of ZDCs. We demonstrate spectator neutron asymmetry can be used to disentangle flow background from the signals of CME. We find that the correlation between projected B -field and ellipticity by varying centrality is different from the one obtained by varying spectator neutron asymmetry. The difference in the nature of these two correlations can be used to dis-

entangle the signals of CME from flow. An experimental confirmation on the studies presented here will lead to a strong support for CME.

This new method to constrain the initial state geometry could be a crucial input for various studies. The main advantage of spectator asymmetry is that it is not affected by the evolution of the system and the final state interactions. This will allow us to perform precision studies of the influence of the initial state geometry on the

hydrodynamic response of the fireball [22, 31], jet suppression etc [32–34].

Acknowledgement: We acknowledge our discussions with R. Haque, H. Masui, B. Mohanty, P. Sorensen and G. Wang. We are grateful to B. Schenke for his comments on the manuscript. The DRONA and PRAFULLA clusters of Computer Division and the LHC grid computing centre at the Variable Energy Cyclotron Centre, supported by the Department of Atomic Energy, Government of India are acknowledged.

-
- [1] D. Kharzeev, R. Pisarski, and M. H. Tytgat, Phys.Rev.Lett. **81**, 512 (1998), arXiv:hep-ph/9804221 [hep-ph].
- [2] D. Kharzeev, Phys.Lett. **B633**, 260 (2006), arXiv:hep-ph/0406125 [hep-ph].
- [3] D. E. Kharzeev, L. D. McLerran, and H. J. Warringa, Nucl.Phys. **A803**, 227 (2008), arXiv:0711.0950 [hep-ph].
- [4] V. Skokov, A. Y. Illarionov, and V. Toneev, Int.J.Mod.Phys. **A24**, 5925 (2009), arXiv:0907.1396 [nucl-th].
- [5] A. Bzdak and V. Skokov, Phys.Lett. **B710**, 171 (2012), arXiv:1111.1949 [hep-ph].
- [6] K. Fukushima, D. E. Kharzeev, and H. J. Warringa, Phys.Rev. **D78**, 074033 (2008), arXiv:0808.3382 [hep-ph].
- [7] S. Pratt, S. Schlichting, and S. Gavin, Phys.Rev. **C84**, 024909 (2011), arXiv:1011.6053 [nucl-th].
- [8] S. A. Voloshin, Phys.Rev. **C70**, 057901 (2004), arXiv:hep-ph/0406311 [hep-ph].
- [9] L. Adamczyk *et al.* (STAR Collaboration), Phys.Rev.Lett. **113**, 052302 (2014), arXiv:1404.1433 [nucl-ex].
- [10] B. Abelev *et al.* (ALICE Collaboration), Phys.Rev.Lett. **110**, 012301 (2013), arXiv:1207.0900 [nucl-ex].
- [11] B. Abelev *et al.* (STAR Collaboration), Phys.Rev. **C81**, 054908 (2010), arXiv:0909.1717 [nucl-ex].
- [12] B. Abelev *et al.* (STAR Collaboration), Phys.Rev.Lett. **103**, 251601 (2009), arXiv:0909.1739 [nucl-ex].
- [13] A. Bzdak, V. Koch, and J. Liao, Phys.Rev. **C81**, 031901 (2010), arXiv:0912.5050 [nucl-th].
- [14] S. A. Voloshin, Phys.Rev.Lett. **105**, 172301 (2010), arXiv:1006.1020 [nucl-th].
- [15] A. Bzdak, Phys.Rev. **C85**, 044919 (2012), arXiv:1112.4066 [nucl-th].
- [16] H. Masui, B. Mohanty, and N. Xu, Phys.Lett. **B679**, 440 (2009), arXiv:0907.0202 [nucl-th].
- [17] T. Hirano, P. Huovinen, and Y. Nara, Phys.Rev. **C83**, 021902 (2011), arXiv:1010.6222 [nucl-th].
- [18] M. R. Haque, Z.-W. Lin, and B. Mohanty, Phys.Rev. **C85**, 034905 (2012), arXiv:1112.2340 [nucl-ex].
- [19] G. Wang and the Star Collaboration, Journal of Physics: Conference Series **230**, 012020 (2010).
- [20] B. Schenke, P. Tribedy, and R. Venugopalan, Phys.Rev. **C89**, 064908 (2014), arXiv:1403.2232 [nucl-th].
- [21] B. Alver and G. Roland, Phys. Rev. C **81**, 054905 (2010).
- [22] D. Teaney and L. Yan, Phys.Rev. **C83**, 064904 (2011), arXiv:1010.1876 [nucl-th].
- [23] G.-Y. Qin, H. Petersen, S. A. Bass, and B. Muller, Phys.Rev. **C82**, 064903 (2010), arXiv:1009.1847 [nucl-th].
- [24] Z. Qiu and U. Heinz, Phys.Lett. **B717**, 261 (2012), arXiv:1208.1200 [nucl-th].
- [25] J. Błoczyński, X.-G. Huang, X. Zhang, and J. Liao, Phys.Lett. **B718**, 1529 (2013), arXiv:1209.6594 [nucl-th].
- [26] J. Błoczyński, X.-G. Huang, X. Zhang, and J. Liao, (2013), arXiv:1311.5451 [nucl-th].
- [27] L. Landau and E. M. Lifshitz, The Classical Theory of Fields, Oxford, England: Pergamon Press, (1984).
- [28] W.-T. Deng and X.-G. Huang, Phys.Rev. **C85**, 044907 (2012), arXiv:1201.5108 [nucl-th].
- [29] Z. Qiu and U. W. Heinz, Phys.Rev. **C84**, 024911 (2011), arXiv:1104.0650 [nucl-th].
- [30] B. Schenke, P. Tribedy, and R. Venugopalan, Nucl.Phys. **A926**, 102 (2014), arXiv:1312.5588 [hep-ph].
- [31] R. S. Bhalerao, M. Luzum, and J.-Y. Ollitrault, Phys.Rev. **C84**, 054901 (2011), arXiv:1107.5485 [nucl-th].
- [32] U. W. Heinz and A. Kuhlman, Phys.Rev.Lett. **94**, 132301 (2005), arXiv:nucl-th/0411054 [nucl-th].
- [33] X. Zhang and J. Liao, Phys.Rev. **C89**, 014907 (2014), arXiv:1208.6361 [nucl-th].
- [34] X. Zhang and J. Liao, Phys. Rev. C **87**, **044910**, 044910 (2013), arXiv:1210.1245 [nucl-th].